Discovery of Aryl Sulfonamides as Isoform-Selective Inhibitors of Na_V1.7 with Efficacy in Rodent Pain Models

Thilo Focken,*,[†] Shifeng Liu,[†,‖] Navjot Chahal,[†] Maxim Dauphinais,[†,§] Michael E. Grimwood,[†] Sultan Chowdhury,[†] Ivan Hemeon,[†] Paul Bichler,[†] David Bogucki,[†] Matthew Waldbrook,[†] Girish Bankar,[†] Luis E. Sojo,[†] Clint Young,[†] Sophia Lin,[†] Noah Shuart,[†] Rainbow Kwan,[†] Jodie Pang,[‡] Jae H. Chang,[‡] Brian S. Safina,[‡] Daniel P. Sutherlin,[‡] J. P. Johnson, Jr.,[†] Christoph M. Dehnhardt,[†] Tarek S. Mansour,[†,⊥] Renata M. Oballa,[†,#] Charles J. Cohen,[†] and C. Lee Robinette[†]

[†]Xenon Pharmaceuticals, Inc., 200-3650 Gilmore Way, Burnaby, BC V5G 4W8, Canada
[‡]Genentech, Inc., 1 DNA Way, South San Francisco, California 94080, United States

S *Supporting Information*

ABSTRACT: We report on a novel series of aryl sulfonamides that act as nanomolar potent, isoform-selective inhibitors of the human sodium channel hNa_V1.7. The optimization of these inhibitors is described. We aimed to improve potency against hNa_V1.7 while minimizing off-target safety concerns and generated compound **3**. This agent displayed significant analgesic effects in rodent models of acute and inflammatory pain and demonstrated that binding to the voltage sensor domain 4 site of Na_V1.7 leads to an analgesic effect *in vivo*. Our findings corroborate the importance of hNa_V1.7 as a drug target for the treatment of pain.


KEYWORDS: *Sodium channel, Na_V1.7, Na_V1.5, pain, aryl sulfonamide, formalin model, cold allodynia*

The sodium channel Na_V1.7 belongs to a family of transmembrane voltage gated sodium channels, which consists of nine isoforms in mammals (Na_V1.1 to Na_V1.9).[1−4] Na_V1.7 plays a crucial role in pain sensation, and there is strong genetic evidence linking Na_V1.7 and its encoding *SCN9A* gene to painful disorders in humans. Gain-of-function mutations in the *SCN9A* gene result in painful conditions such as inherited erythromelalgia, paroxysmal extreme pain disorder, and idiopathic small fiber neuropathies. In contrast, loss-of-function mutations in the *SCN9A* gene were found to be the genetic cause of a rare disorder called congenital insensitivity to pain, characterized by a complete loss of the ability to sense painful stimuli. It is noteworthy that no significant side effects have been reported in people lacking Na_V1.7, such as cognitive, motor, or non-nociceptive sensory impairments other than anosmia, giving further support to the concept of Na_V1.7 antagonists as analgesics.[1−4] The predominant expression of the Na_V1.7 isoform in the PNS may offer a pathway to limit CNS-related adverse effects by developing compounds that do not cross the blood−brain barrier.[2]

Combined, these observations and findings have made Na_V1.7 a promising target for drug development for the treatment of pain. Indeed, there has been tremendous interest in the development of small molecule Na_V1.7 inhibitors as analgesics, particularly isoform-selective inhibitors, and coverage of the progress has been the subject of several excellent reviews.[1−7] In recent years, a series of aryl sulfonamides as Na_V inhibitors have been reported that appear to be highly selective for Na_V1.7 over the cardiac ion channel Na_V1.5.[4−6,8]

Since block of the Na_V1.5 channel may lead to arrhythmia and thus limit the therapeutic potential of nonselective Na_V1.7 inhibitors, isoform-selective inhibitors have attracted considerable interest due to their potential to avoid these adverse events.[3,5] An example is aryl sulfonamide PF-04856264 (Figure 1), which selectively blocks Na_V1.7 over Na_V1.5 and Na_V1.3.
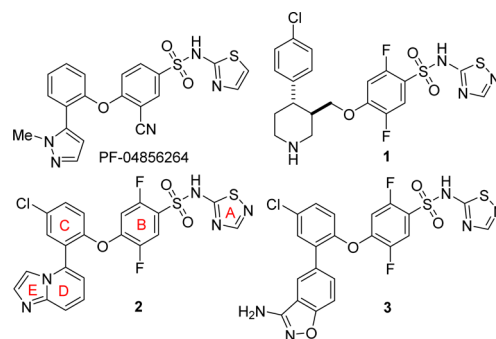
Figure 1. Structures of selected aryl sulfonamides as Na_V1.7 inhibitors and ring nomenclature.

This class of compounds reportedly binds to a unique site in the voltage sensor domain 4 (VSD4) of $Na_V1.7$, which is distinct from the pore binding sites of tetrodotoxin or local anesthetics.[4,8] We recently obtained the crystal structure of a chimera consisting of human $Na_V1.7$ VSD4 and a bacterial pore domain in complex with an aryl sulfonamide.[9]

However, block of $hNa_V1.7$ through VSD4 is very steeply state-dependent such that block is much weaker when channel opening is elicited from cells that are hyperpolarized, as discussed later.[8,9] It remained uncertain if binding to VSD4 in this manner would result in analgesic activity. Although there is ample evidence that nonselective Na_V pore blockers act as analgesics,[1−7] no published reports have demonstrated the same for $Na_V1.7$ VSD4 inhibitors.

We have had a long-standing interest in developing $Na_V1.7$ blockers[10−12] and published on the discovery of piperidine scaffold 1, with excellent selectivity for $Na_V1.7$ over $Na_V1.5$.[13] Although this series of compounds yielded potent $hNa_V1.7$ blockers, its zwitterionic character was believed to contribute to the poor PK properties that prevented the use of these compounds in preclinical proof-of-concept studies. Therefore, we explored related scaffolds that would provide better PK properties while retaining the potency and selectivity profile of 1 and allow us to conduct in vivo efficacy studies to probe if binding to VSD4 of $Na_V1.7$ leads to an analgesic effect. We identified a novel biaryl ether sulfonamide scaffold containing a fused heterobicyclic D/E ring system that we considered suitable for further exploration and imidazo[1,2-a]pyridine 2 emerged as a lead (Figure 1) with an IC_{50} of 17 nM for the inhibition of $hNa_V1.7$ as determined by a voltage-clamp assay. Herein, we report our optimization efforts that led to the discovery of subtype-selective $Na_V1.7$ blocker 3, a tool compound that demonstrated significant in vivo efficacy in preclinical proof-of-concept studies.

The general synthetic route to prepare these compounds is outlined in Scheme 1 using isoxazole 3 as a typical example. In most cases, a convergent approach was employed that involved the Suzuki−Miyaura coupling of a fused bicyclic D/E ring halide with a C-ring hydroxyphenyl boronic acid, followed by connection to an A−B ring building block via S_NAr reaction and global deprotection (for ring numbering see Figure 1). The synthesis of 3 started with the conversion of commercially available 5-bromobenzo[d]isoxazol-3-amine into its Boc derivative 5. Alternatively, 5 was easily prepared from 4 in two steps through reaction with N-hydroxyacetamide and potassium tert-butoxide, followed by treatment with strong acid. Compound 5 was then coupled with (5-chloro-2-hydroxyphenyl)boronic acid under Suzuki−Miyaura conditions to afford phenol 6. Nucleophilic aromatic substitution of trifluorobenzenesulfonamide 9, prepared in two steps from 7 and 2,4,5-trifluorobenzenesulfonyl chloride, with phenol 6 and subsequent global deprotection afforded isoxazole 3. Conversion into its sodium salt 3a was performed by treatment with NaOH in methanol.

The correct positioning of heteroatoms in the fused heterocycles proved to be crucial for improving potency of this series of aryl sulfonamides (Table 1). While 6,5-fused 2 showed good potency against $Na_V1.7$, its 5,6-fused analogue imidazo[1,5-a]pyrazine 12 was inactive. Rearranging and partially saturating the fused D/E ring system led to tetrahydroimidazo[1,2-a]pyrazine 13 and a 10-fold improvement in potency compared to 12. Although we mainly focused on 6,5-fused bicyclic ring systems in our optimization strategy,

Scheme 1. General Synthetic Route of Biarylether Sulfonamides Exemplified with Benzisoxazole 3[a]
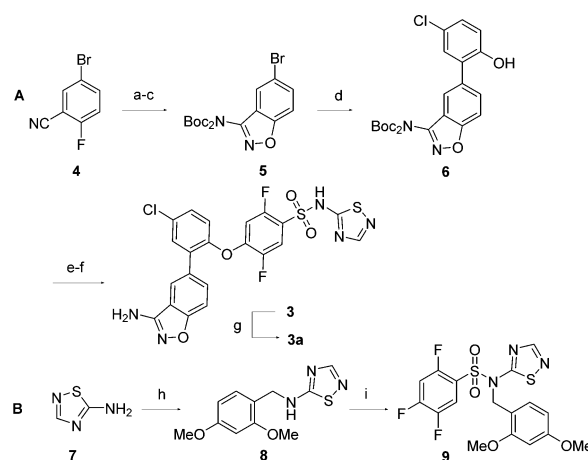
[a]Reagents and conditions: (a) N-hydroxyacetamide, t-BuOK, DMF, 99%; (b) TFA, conc. HCl, reflux, 93%; (c) di-tert-butyl dicarbonate, DMAP, CH_2Cl_2, 58%; (d) (5-chloro-2-hydroxyphenyl)boronic acid, $Pd(PPh_3)_4$, Na_2CO_3 (2 M), DME, reflux, 63%; (e) 9, K_2CO_3, DMSO, 55%; (f) TFA, CH_2Cl_2, 63%; (g) NaOH, MeOH, 96%. (h) (1) 2,4-dimethoxybenzaldehyde, toluene, Dean−Stark, reflux, (2) $NaBH_4$, MeOH, 59%; (i) 2,4,5-trifluorobenzenesulfonyl chloride, $LiN(TMS)_2$, THF, −78 °C, 84%.

Table 1. SAR of the Fused D/E Bicycle

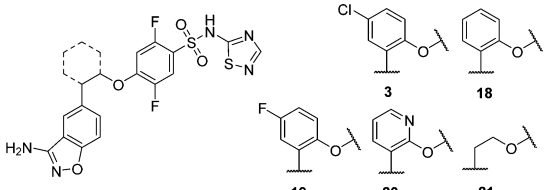| cmpd	$hNa_V1.7$ IC_{50} [nM][a]	$hNa_V1.5$ IC_{50} [nM][a]
2	17 ± 6	>10000
3	0.4 ± 0.2	1380 ± 668
10	0.5 ± 0.0	230 ± 42
11	5.3 ± 2.1	>10000[b]
12	2300 ± 870	nd
13	222 ± 54	>10000[b]
14	3.6 ± 2.0	>10000
15	1.7 ± 0.9	>10000[b]
16	0.3 ± 0.2	>10000
17	1.7 ± 0.5	>10000

[a]IC_{50} values are reported as mean ± SD, generated on an automated voltage-clamp platform; nd, not determined. [b]IC_{50} generated from fit of pooled data; SD not applicable.

we also tested 6,6-fused rings, such as quinoxaline 14, which displayed high potency against $Na_V1.7$ and excellent selectivity over $Na_V1.5$ (>2700-fold). Its 6,5-fused analogue benzimidazole 15 performed slightly better, with an IC_{50} of 1.7 nM against $Na_V1.7$. Adding an amino group to 15 provided 16, which showed a further 6-fold boost in potency. Replacement of the 2-aminobenzimidazole moiety in 16 by a benzimidazolone gave

17, which maintained potency relative to 15, though it was considerably less active than 16. Rearrangement of 16 to isomeric 3-aminoindazole 11 resulted in a 17-fold drop in potency. Gratifyingly, replacement of one of the indazole nitrogens by an oxygen led to a significant boost in potency and isoxazole 3 showed excellent potency against $hNa_V1.7$ with an IC_{50} of 0.4 nM. Adding a methyl group to give 10 had no significant impact on the potency against $Na_V1.7$. In contrast, the additional methyl group caused a gain in potency against $Na_V1.5$, resulting in a decrease in selectivity against this isoform.

We next turned our attention to modifications of the C-ring (Table 2). Changing the C-ring from chlorophenyl as in 3 to

Table 2. SAR for the Optimization of the C-Ring

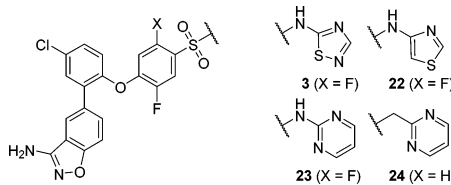| cmpd	$hNa_V1.7$ IC_{50} [nM][a]	cmpd	$hNa_V1.7$ IC_{50} [nM][a]
3	0.4 ± 0.2	20	51 ± 11
18	3.0 ± 0.8	21	241 ± 122
19	1.7 ± 0.4		

[a]IC_{50} values are reported as mean ± SD, generated on an automated voltage-clamp platform.

less lipophilic phenyl 18 or fluorophenyl 19 led to a drop in potency. The introduction of a heteroatom was not tolerated, and 20 showed a 17-fold decrease in activity relative to 18. The biaryl ether hinge motif is critical for potency. Indeed, replacement of the C-ring with an aliphatic linker gave 21, which was 80-fold less potent than 18.

The sulfonamide moiety and the heterocyclic A-ring form the acidic "warhead" of the molecules (measured pK_a for 3: 3.2), which is vital for binding to the protein, presumably via a salt-bridge to a positively charged residue such as arginine.[8,9] In particular, the thiadiazole group was optimal in terms of potency, as other heteroaromatic rings typically led to a >10-fold decrease in blockage of $Na_V1.7$ (Table 3). Replacement of the sulfonamide nitrogen by a methylene group to provide sulfone 24 was not tolerated and resulted in a complete loss of potency.

Early safety assessment included monitoring for potential liabilities such as inhibition of the cardiac ion channels $hNa_V1.5$

Table 3. SAR for the Heterocyclic A-Ring

cmpd	$hNa_V1.7$ IC_{50} [nM][a]	cmpd	$hNa_V1.7$ IC_{50} [nM][a]
3	0.4 ± 0.2	23	4.4 ± 0.9
22	8.7 ± 3.6	24	5200[b]

[a]IC_{50} values are reported as mean ± SD, generated on an automated voltage-clamp platform. [b]IC_{50} generated from fit of pooled data; SD not applicable.

and hERG and CYP enzymes. In addition to having excellent selectivity for $hNa_V1.7$ over $hNa_V1.5$, none of the compounds 2−23 showed significant blockage of the hERG channel, with less than 11% inhibition at 5 μM, as measured by displacement of [³H]astemizole. However, compounds 2−21 containing a thiadiazole A-ring showed significant inhibition of the CYP isoforms 2C9 and 3A4. Thus, 3 inhibited CYP2C9 and CYP3A4 with an IC_{50} of 0.17 and 0.077 μM, respectively. Conversely, only weak inhibition of the isoforms 1A2 and 2D6 was observed in this series (IC_{50}s 9 to >10 μM). Structural modifications of the B, C, and D/E ring systems had little effect on the inhibition of the CYPs. As previously observed during our optimization efforts of piperidine scaffold 1 (Figure 1),[13] the affinity for the CYPs was dependent on the heterocyclic A-ring, in particular the inhibition of CYP3A4. For instance, pyrimidine 23 showed an improved CYP profile relative to 3, with reduced inhibition of CYP2C9 (IC_{50} 0.57 μM), and no inhibition of the CYPs 2C19, 1A2, 2D6, and 3A4 (>10 μM for 23). We were cognizant of the potential impact of the CYP liabilities on further development. Nevertheless, we were interested in studying these compounds in rodent pain models in order to probe if blocking $Na_V1.7$ would translate to *in vivo* efficacy. Thus, selected compounds were further characterized by voltage-clamp against a panel of human and rodent Na_V isoforms.

Compound 3 showed potent blockage of human $Na_V1.7$ with high selectivity for the inhibition of $Na_V1.7$ over the subtypes $hNa_V1.1$ and $hNa_V1.5$ (Table 4). However, it showed only 10-

Table 4. Inhibition of Human $Na_V1.x$ Isoforms for Compounds 3 and 16 and Rodent $Na_V1.7$ Orthologs for 3

$Na_V1.x$	cmpd 3 IC_{50} [nM][a]	cmpd 16 IC_{50} [nM][a]
hNa_V 1.1	3080 ± 1850	6380 ± 3900
hNa_V 1.2	4.2 ± 2.3	0.2 ± 0.0
hNa_V 1.3	nd	9330 ± 4590
hNa_V 1.4	nd	>10000[c]
hNa_V 1.5	1380 ± 668	>10000
hNa_V 1.6	11 ± 4	0.8 ± 0.7
hNa_V 1.7	0.4 ± 0.2	0.3 ± 0.2
hNa_V 1.8[b]	nd	3850 ± 930
$rNa_V1.7$	26 ± 10	nd
$mNa_V1.7$	0.2 ± 0.1	nd

[a]IC_{50} values are reported as mean ± SD, generated on an automated voltage-clamp platform; nd, not determined. [b]Determined by manual voltage-clamp. [c]IC_{50} generated from fit of pooled data; SD not applicable.

fold and 27-fold selectivity against the human subtypes $Na_V1.2$ and $Na_V1.6$, respectively. In addition to blocking the human $Na_V1.7$ isoform, 3 also displayed comparably potent inhibition of mouse $Na_V1.7$. Notably, inhibition of the rat ortholog by 3 was >60-fold less potent than for the human isoform. Analogues of 3 showed comparable high selectivity for $hNa_V1.7$ over the rat isoform, and in many cases, the $rNa_V1.7$ potency was inadequate for use in efficacy studies. Thus, quinoxaline 14 showed >200-fold weaker inhibition for $rNa_V1.7$ (IC_{50} 740 nM) than $hNa_V1.7$ (Table 1). Compound 16 had a similar electrophysiology profile as 3 (Table 4), with high affinity for human $Na_V1.7$, $Na_V1.2$, and $Na_V1.6$ and high selectivity over $hNa_V1.1$, $hNa_V1.3$, $hNa_V1.5$, and $hNa_V1.8$ (>12000-fold). In addition to molecular selectivity, the aryl

Table 5. In vitro DMPK profile for 3 and pharmacokinetic parameters for 3 in rats.[a]

|	Sol.[b,c]		CL$_{hep}$ HH/MH/RH[c,d]		P$_{app}$/MDR1[c,e]	rPPB[f]
	121		13/65/36		2.1/47	98.9 ± 1.1
dose (mpk, route)	C$_{max}$ (μM)	T$_{max}$ (h)	AUC$_{0-inf}$ (μM·h)	T$_{1/2}$ (h)	CL$_p$ (mL/min/kg)	V$_{ss}$ (L/kg)
1, iv	2.9 ± 0.2	N/A	0.18 ± 0.01	0.13 ± 0.01	177 ± 12	1.4 ± 0.1
20, ip	5.3 ± 1.7	0.06 ± 0.04	13.5 ± 0.0	2.2 ± 0.5	N/A	N/A

[a]Rat PK data is mean ± SD. [b]Kinetic solubility (μM) at pH 7.2. [c]SD not applicable. [d]Predicted hepatic clearance (mL/min/kg). [e]Apparent permeability (10^{-6} cm/s), apical to basolateral side (A to B), and MDR1 efflux ratio. [f]Plasma protein binding in rat ± SD.

sulfonamides in this series also showed high functional selectivity that derives from steeply state-dependent block of hNa$_V$1.7 and preferred binding to inactivated channels.[8,9] Thus, **16** inhibited hNa$_V$1.7 with an IC$_{50}$ of 0.3 nM when binding equilibrated at −60 mV (favoring the inactivated state, Table 4), whereas the IC$_{50}$ was 495 nM when binding equilibrated at −150 mV (favoring the rested state). This state-dependent block should result in a preference for blocking depolarized and rapidly firing cells assumed to occur in disease conditions.[7]

The in vitro DMPK profile (Table 5) for **3** was satisfactory with predicted moderate hepatic clearance in human and rat based upon studies with hepatocytes, and marginally higher clearance in mouse. Permeability was low to moderate, and a high MDR1 efflux ratio was measured. Plasma protein binding was very high in rat with a free fraction of ∼1.1% for **3**. The in vivo PK parameters for compound **3** in rats are summarized in Table 5. Following iv dosing of **3**, half-life (t$_{1/2}$) was short and plasma clearance was high and above the rat hepatic blood flow, suggesting contribution from extrahepatic clearance pathways. Oral dosing (po) showed poor exposure. Fortunately, intraperitoneal (ip) administration provided sufficient exposure to allow us to study target engagement. At 20 mpk, ip dosing gave a 7-fold higher exposure than po dosing. Despite the high plasma concentration, brain penetration remained low with a brain-to-plasma ratio of 0.019, consistent with the high MDR1 efflux ratio measured in vitro. Based on the combination of its superior rodent Na$_V$1.7 potency and PK profile in comparison to other analogues, compound **3** was chosen for further evaluation in animal models for nociceptive pain. Compound **16** was not progressed due to its poor aqueous solubility.

We initially selected a formalin- and an aconitine-induced pain model in rats to probe for analgesic effects. The formalin inflammatory pain model utilizes formalin as a pain-inducing agent and generates a biphasic pain response.[14] The first phase lasts from 0 to 9 min (phase 1 in Figure 2A) and is believed to result from direct stimulation of nociceptors by formalin, whereas the second phase from 10 to 60 min (phases 2a and 2b) includes an inflammatory pain response to formalin. The aconitine acute pain assay is a target-engagement model developed in-house that employs aconitine, a powerful neurotoxin and sodium channel activator that promotes channel opening and inhibits transitioning into the inactivated state, thus stimulating a pain response.[15] In both assays, compound **3** was dosed as its sodium salt **3a** by ip injection.

As depicted in Figure 2A, isoxazole **3** showed a reduction of the pain response in phase 2a of the formalin assay in a dose-dependent manner. Though it was ineffective at a dose of 30 mpk, it significantly decreased nociceptive behavior at 100 mpk compared to controls (60% reduction relative to formalin). Furthermore, **3** (100 mpk dose) caused a delay of onset of the pain response and shifted it to phase 2b of the assay, showing an increase in nociceptive behavior in this phase compared to controls. We next evaluated compound **3** at ip doses of 30 and
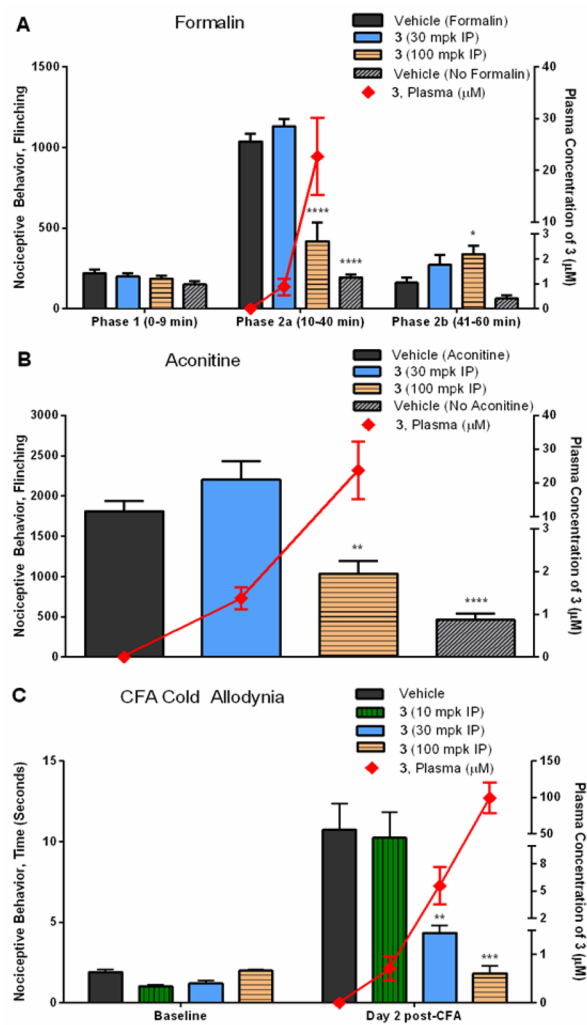
Figure 2. (A) Effect of **3** on formalin-induced pain in rats, binned by phases. (B) Effect of **3** on aconitine-induced pain in rats summed over 60 min. (C) Effect of **3** on CFA-induced cold allodynia in mice. Terminal plasma concentrations of **3** are shown. Data are presented as mean ± SEM (n = 6−8 animals/group). Statistical analysis was performed with a two-way ANOVA, followed by a Bonferroni posthoc test (formalin assay) or by a one-way ANOVA, followed by a Dunnett's posthoc test (aconitine and cold allodynia): *p < 0.05; **p < 0.01; ***p < 0.001 vs vehicle.

100 mpk, respectively, for effects on acute pain sensitivity in rats using aconitine as pain stimulus. At the lower dose, no change in pain behavior relative to vehicle alone was observed. However, the higher dose produced a substantial inhibition of the pain response (43% compared to the aconitine control, Figure 2B). In both rat pain models, **3** showed efficacy at free plasma concentrations of about 250−260 nM.

Encouraged by these results, we tested **3** in a complete Freund's adjuvant (CFA) induced cold allodynia assay in mice.[16] Following intraplantar injection of CFA in the left hind paw, inflammation develops in the affected (ipsilateral) hind paw. On day 2 after CFA administration, mice received an ip dose of either test compound **3** (as Na-salt **3a**) or the vehicle. Cold sensitivity pain was induced by evaporation of acetone, which was applied directly to the plantar surface of the ipsilateral hind paw. Compound **3** displayed a dose-dependent reduction of the pain response (Figure 2C). At the lowest dose of 10 mpk, no change in pain behavior relative to vehicle was observed. In comparison, the higher doses significantly reduced nociceptive behavior, with 59% reduction at the 30 mpk dose and reduction close to baseline at the 100 mpk dose (83% compared to vehicle).

Combined, the data from our efficacy studies demonstrate that $Na_V1.7$ inhibitor **3** markedly attenuates pain sensation in rodent models of acute and inflammatory pain and indicates *in vivo* target engagement of sodium channels. Though compound **3** displayed high selectivity for $hNa_V1.7$ over other human isoforms, the selectivity profile in other species remains to be investigated. Thus, we cannot rule out a contribution of other sodium channel isoforms associated with sensation of pain, such as $Na_V1.6$[17] or $Na_V1.8$,[4,18] to the observed analgesic effect in rodents. Existing data from animal studies with a $Na_V1.7$-selective monoclonal antibody however suggest that inhibition of $Na_V1.7$ alone is sufficient to produce an analgesic effect.[19] In addition, results from a formalin study with $Na_V1.7$ DRG-null mice ($Na_V1.7R^{-/-}$) showing a reduced pain response further validate the major role of $Na_V1.7$ in acute and inflammatory pain.[20,21]

In summary, we have described the discovery and optimization of a novel series of aryl sulfonamides as potent and isoform-selective $Na_V1.7$ inhibitors. Our compounds show exquisite selectivity over the human sodium channel isoforms $Na_V1.1$, $Na_V1.3$, $Na_V1.5$, and $Na_V1.8$ as determined by voltage-clamp electrophysiology, but less selectivity against $Na_V1.2$ and $Na_V1.6$. Compound **3** displayed significant analgesic effects in rodent models of acute and inflammatory pain and demonstrated that highly plasma protein bound aryl sulfonamides can display meaningful target engagement *in vivo*. In addition, we were able to validate that targeting the VSD4 of $Na_V1.7$ leads to an analgesic effect *in vivo*. Our findings support the notion of $Na_V1.7$ as an important mediator of the pain response and should augment the current high interest in developing isoform-selective $Na_V1.7$ inhibitors as analgesics. The observed isoform selectivity against myocardial $Na_V1.5$ presents a highly desirable safety advantage. In addition, the low CNS exposure may minimize adverse events putatively arising from block of CNS sodium channels and thereby mitigate potentially potent block of $Na_V1.6$ and $Na_V1.2$.[2] Further optimization of PK properties and CYP inhibition is desirable and will focus on the heterocyclic A- and D/E-ring systems.

ASSOCIATED CONTENT

ⓈSupporting Information

The Supporting Information is available free of charge on the ACS Publications website at DOI: 10.1021/acsmedchemlett.5b00447.

   Synthetic procedures and NMR spectra of all final compounds, and description of the *in vitro* assays and rodent pain models (PDF)

AUTHOR INFORMATION

Corresponding Author
*E-mail: tfocken@xenon-pharma.com.

Present Addresses
‖Hangzhou Yingchuang Pharma, Longtan Road No. 20, Yuhang District, Hangzhou, Zhejiang, 31121, P. R. China.
§Department of Chemistry, Université de Montréal, PO Box 6128, Station Downtown, Montreal, QC H3C 3J7, Canada.
⊥Sabila Biosciences LLC, 5 Overlook Road, New City, New York 10956, United States.
#Inception Sciences Canada, 887 Great Northern Way, Suite 210, Vancouver, BC V5T 4T5, Canada.

Author Contributions
All authors have given approval to the final version of the manuscript.

Notes
The authors declare the following competing financial interest(s): Both Xenon Pharmaceuticals and Genentech are actively developing $Na_V1.7$ inhibitors as therapeutic agents.

ABBREVIATIONS

ANOVA, analysis of variance; CFA, complete Freund's adjuvant; CL_{hep}, predicated hepatic clearance; CL_p, plasma clearance; C_{max}, maximum concentration; DRG, dorsal root ganglion; HH, human hepatocytes; MDR1, multidrug resistance protein 1; MH, mouse hepatocytes; mpk, milligram per kilogram; h/m/r Na_V, human/mouse/rat voltage-gated sodium channel; P_{app}, apparent permeability; RH, rat hepatocytes; SD, standard deviation; SEM, standard error of the mean; T_{max}, time of maximum concentration; V_{ss}, volume of distribution; VSD, voltage sensor domain

REFERENCES

(1) Dib-Hajj, S. D.; Yang, Y.; Black, J. A.; Waxman, S. G. The $Na_V1.7$ Sodium Channel: From Molecule to Man. *Nat. Rev. Neurosci.* **2013**, *14*, 49−62.

(2) Eijkelkamp, N.; Linley, J. E.; Baker, M. D.; Minett, M. S.; Cregg, R.; Werdehausen, R.; Rugiero, F.; Wood, J. N. Neurological Perspectives on Voltage-Gated Sodium Channels. *Brain* **2012**, *135*, 2585−2612.

(3) England, S.; Rawson, D. Isoform-Selective Voltage-Gated Na+ Modulators as Next-Generation Analgesics. *Future Med. Chem.* **2010**, *2*, 775−790.

(4) de Lera Ruiz, M.; Kraus, R. L. Voltage-Gated Sodium Channels: Structure, Function, Pharmacology, and Clinical Indications. *J. Med. Chem.* **2015**, *58*, 7093−7118.

(5) Sun, S.; Cohen, C. J.; Dehnhardt, C. M. Inhibitors of Voltage-Gated Sodium Channel $Na_V1.7$: Patent Applications Since 2010. *Pharm. Pat. Anal.* **2014**, *3*, 509−521.

(6) Bagal, S. K.; Chapman, M. L.; Marron, B. E.; Prime, R.; Storer, R. I.; Swain, N. A. Recent Progress in Sodium Channel Modulators for Pain. *Bioorg. Med. Chem. Lett.* **2014**, *24*, 3690−3699.

(7) Nardi, A.; Damann, N.; Hertrampf, T.; Kless, A. Advances in Targeting Voltage Gated Sodium Channels with Small Molecules. *ChemMedChem* **2012**, *7*, 1712−1740.

(8) McCormack, K.; Santos, S.; Chapman, M. L.; Krafte, D. S.; Marron, B. E.; West, C. W.; Krambis, M. J.; Antonio, B. M.; Zellmer, S. G.; Printzenhoff, D.; Padilla, K. M.; Lin, Z.; Wagoner, P. K.; Swain, N. A.; Stupple, P. A.; de Groot, M.; Butt, R. P.; Castle, N. A. Voltage Sensor Interaction Site for Selective Small Molecule Inhibitors of Voltage-Gated Sodium Channels. *Proc. Natl. Acad. Sci. U. S. A.* **2013**, *110*, E2724−E2732.

(9) Ahuja, S.; Mukund, S.; Deng, L.; Khakh, K.; Chang, E.; Ho, H.; Shriver, S.; Young, C.; Lin, S.; Johnson, J. P., Jr.; Wu, P.; Li, J.; Coons, M.; Tam, C.; Brillantes, B.; Sampang, H.; Mortara, K.; Grimwood, M.;

Dehnhardt, C.; Andrez, J.-C.; Focken, T.; Sutherlin, D. P.; Safina, B. S.; Starovasnik, M. A.; Ortwine, D. F.; Franke, Y.; Cohen, C. J.; Hackos, D. H.; Koth, C. M.; Payandeh, J. Structural basis of Na$_V$1.7 inhibition by an isoform-selective small molecule antagonist. *Science* **2015**, *350*, aac5464.

(10) Chowdhury, S.; Liu, S.; Cadieux, J. A.; Hsieh, T.; Chafeev, M.; Sun, S.; Jia, Q.; Sun, J.; Wood, M.; Langille, J.; Sviridov, S.; Fu, J.; Zhang, Z.; Chui, R.; Wang, A.; Cheng, X.; Zhong, J.; Hossain, S.; Khakh, K.; Rajlic, I.; Verschoof, H.; Kwan, R.; Young, W. Tetracyclic Spirooxindole Blockers of hNa$_V$1.7: Activity in Vitro and in CFA-Induced Inflammatory Pain Model. *Med. Chem. Res.* **2013**, *22*, 1825−1836.

(11) Goldberg, Y. P.; Price, N.; Namdari, R.; Cohen, C. J.; Lamers, M. H.; Winters, C.; Price, J.; Young, C. E.; Verschoof, H.; Sherrington, R.; Pimstone, S. N.; Hayden, M. R. Treatment of Na$_V$1.7-Mediated Pain in Inherited Erythromelalgia Using a Novel Sodium Channel Blocker. *Pain* **2012**, *153*, 80−85.

(12) Chowdhury, S.; Chafeev, M.; Liu, S.; Sun, J.; Raina, V.; Chui, R.; Young, W.; Kwan, R.; Fu, J.; Cadieu, J. A. Discovery of XEN907, a Spirooxindole Blocker of Na$_V$1.7 for the Treatment of Pain. *Bioorg. Med. Chem. Lett.* **2011**, *21*, 3676−3681.

(13) Sun, S.; Jia, Q.; Zenova, A. Y.; Chafeev, M.; Zhang, Z.; Lin, S.; Kwan, R.; Grimwood, M. E.; Chowdhury, S.; Young, C.; Cohen, C. J.; Oballa, R. M. The Discovery of Benzenesulfonamide-Based Potent and Selective Inhibitors of Voltage-Gated Sodium Channel Na$_V$1.7. *Bioorg. Med. Chem. Lett.* **2014**, *24*, 4397−4401.

(14) Yaksh, T. L.; Ozaki, G.; McCumber, D.; Rathbun, M.; Svensson, C.; Malkmus, S.; Yaksh, M. C. An Automated Flinch Detecting System for Use in the Formalin Nociceptive Bioassay. *J. Appl. Physiol.* **2001**, *90*, 2386−2402.

(15) Catterall, W. A.; Cestèle, S.; Yarov-Yarovoy, V.; Yu, F. H.; Konoki, K.; Scheuer, T. Voltage-Gated Ion Channels and Gating Modifier Toxins. *Toxicon* **2007**, *49*, 124−141.

(16) Minett, M. S.; Falk, S.; Santana-Varela, S.; Bogdanov, Y. D.; Nassar, M. A.; Heegaard, A. M.; Wood, J. N. Pain Without Nociceptors? Na$_V$1.7-Independent Pain Mechanisms. *Cell Rep.* **2014**, *6*, 301−312.

(17) Sittl, R.; Lambert, A.; Huth, T.; Schuy, E. T.; Link, A. S.; Fleckenstein, J.; Alzheimer, C.; Grafe, P.; Carr, R. W. Anticancer Drug Oxaliplatin Induces Acute Cooling-Aggravated Neuropathy via Sodium Channel Subtype Na$_V$1.6-Resurgent and Persistent Current. *Proc. Natl. Acad. Sci. U. S. A.* **2012**, *109*, 6704−6709.

(18) Jarvis, M. F.; Honore, P.; Shieh, C.-C.; Chapman, M.; Joshi, S.; Zhang, X.-F.; Kort, M.; Carroll, W.; Marron, B.; Atkinson, R.; Thomas, J.; Liu, D.; Krambis, M.; Liu, Y.; McGaraughty, S.; Chu, K.; Roeloffs, R.; Zhong, C.; Mikusa, J. P.; Hernandez, G.; Gauvin, D.; Wade, C.; Zhu, C.; Pai, M.; Scanio, M.; Shi, L.; Drizin, I.; Gregg, R.; Matulenko, M.; Hakeem, A.; Gross, M.; Johnson, M.; Marsh, K.; Wagoner, P. K.; Sullivan, J. P.; Faltynek, C. R.; Krafte, D. S. A-803467, A Potent and Selective Na$_V$1.8 Sodium Channel Blocker, Attenuates Neuropathic and Inflammatory Pain in the Rat. *Proc. Natl. Acad. Sci. U. S. A.* **2007**, *104*, 8520−8525.

(19) Lee, J.-H.; Park, C.-K.; Chen, G.; Han, Q.; Xie, R.-G.; Liu, T.; Ji, R.-R.; Lee, S.-Y. A Monoclonal Antibody That Targets a Na$_V$1.7 Channel Voltage Sensor for Pain and Itch Relief. *Cell* **2014**, *157*, 1393−1404.

(20) Minett, M. S.; Nassar, M. A.; Clark, A. K.; Passmore, G.; Dickenson, A.; Wang, F.; Malcangio, M.; Wood, J. N. Distinct Na$_V$1.7-Dependent Pain Sensations Require Different Sets of Sensory and Sympathetic Neurons. *Nat. Commun.* **2012**, *3*, 791.

(21) Nassar, M. A.; Stirling, L. C.; Forlani, G.; Baker, M. D.; Matthews, E. A.; Dickenson, A. H.; Wood, J. N. Nociceptor-Specific Gene Deletion Reveals a Major Role for Na$_V$1.7 (PN1) in Acute and Inflammatory Pain. *Proc. Natl. Acad. Sci. U. S. A.* **2004**, *101*, 12706−12711.